IOSR Journal of Applied Chemistry (IOSR-JAC)
e-ISSN: 2278-5736.Volume 15, Issue 6 Ser. II (June 2022), PP 10-22
www.iosrjournals.org

Technical Properties and Uses of the Aluminum Hydroxide, Dried, Milled and Classified

Gheorghe Dobra[1], Sorin Iliev[2], Lucian Cotet[2*], Alina Boiangiu[2], Bogdan Stefan Vasile[3,4], Ionela Andreea Neacsu[3,4] Adrian Ionut Nicoara[3,4] Vasile Adrian Surdu[3,4] and Laurentiu Filipescu[3]

[1]*Alro Slatina SA, Slatina, Romania*
[2]*Alum Tulcea SA,, Tulcea, Romania*
[3]*Faculty of Applied Chemistry and Materials Science, UPB Romania, Romania,*
[4]*National Research Center for Micro and Nanomaterials, UPB Bucharest, Romania*
**Corresponding author: Lucian Cotet: lcotet@alum.ro*

Abstract:
For this paper, the dried, milled and particle size classified aluminum hydroxide samples were collected from the new unit, designed to produce different grades of dried and milled aluminum hydroxide with specific particle size distribution at Alum SA Tulcea, Romania. The research program included the selection of several samples based on particle size and particle size distribution, namely, fractions 0-10, 0-20, 0-45 and 45-150 microns, and the normal Bayer product 0-150 microns as blank sample. The thermal treatments of these samples consist in their heating up at a rate of 5ºC/minute at 260°C, 300°C and respectively, 400°C, followed by a 3 hours more heating at each final temperature. In our previous experiments, all the emerging materials have been characterized by measuring their basic properties, as: mass loss during heating, crystalline and amorphous phase composition, BET specific surface, pore size distribution, particle size distribution, dehydroxylation degree, and other minor properties. In this paper, additional information has been added for full characterization of the above materials by measuring the last important technical properties of aluminum hydroxide: water adsorption capacity, oil adsorption capacity, absolute density and whiteness degree.
Background*: Gibbsite $Al(OH)_3$, without any doubt, is the most important product manufactured at industrial scale, among all the hydrated alumina grades. Actually, most of the other hydrates with any industrial uses did come from different quality classes of the gibbsite, or as raw material precursors in different technologies of thermal treatment, from simple calcination up to the hydrothermal conversion. Gibbsite activation is a common way to improve reactivity of the industrial products and to conduct the process to the desired final product or to any requested quality of the products.*
Materials and Methods*. Because one purpose of this paper was to point up the importance of particle size distribution (PSD) in the aluminum hydroxide phase transitions, as well as in their amorphisation process, there have been selected only 4 samples, which can rightly exhibit the large difference between them, in terms of particle sizes and PSD. The samples have been firstly dried at 60°C for 24 h, and then calcined at 260°C, 300°C and respectively, 400°C, under different temperature conditions, in order to obtain low temperature calcined alumina products*
Results. *The new crystalline and amorphous products were characterized by measuring the following properties: particle size dimensions (PSD), crystallinity, density, brightness, water adsorption capacityand oil adsorption capacity. Also, was studied the correlation of these properties with the thermal amorphisation process parameters.*
Conclusions. *This entire study has demonstrated that the final properties of low temperature calcined aluminas are dependent on the following dynamic factors: temperature and rate of heating, initial particles dimension and advanced grinding or intensive mechanical activation.*
Key words*: Calcined aluminas, crystallinity, density, brightness, water adsorption capacity, oil adsorption capacity, particle size dimensions.*

Date of Submission: 08-06-2022 Date of Acceptance: 24-06-2022

I. Introduction

Aluminum hydroxide, as an intermediary wet product (gibbsite, $Al_2O_33H_2O$), is industrially produced by Bayer process from different kinds of bauxite and further converted by calcination into high temperature ceramic alumina or in alumina for metallurgical use. Mainly, the gibbsite quality, particle size, crystallinity and

crystals morphology are strongly influenced by the Bayer process parameters [1-4]. Aluminum hydroxide and its related hydrates are very important materials with various industrial applications, mainly as: adsorbents and water purification reactants [5-9], fire retardants and fillers for plastics and silicon rubber composites [10-15] and coating materials [16-18]. Any of their precursor phases [19-22], as well as the high temperature ceramic oxides [23-25], porous ceramics and castable ceramics [26-27], and low temperature calcined alumina may serve as raw materials for catalysts and catalyst supports [28-32]. All these applications are requiring a long row of specific properties, like pore size and pore size distribution [33,34], a high specific surface area [35–37], and the degree of crystallinity, which also plays an essential role [38–41] in all categories of alumina hydrates related products.

Gibbsite Al(OH)3, without any doubt, is the most important product manufactured at industrial scale, among all the hydrated alumina grades. Actually, most of the other hydrates with any industrial uses did come from different quality classes of the gibbsite, or as raw material precursors in different technologies of thermal treatment, from simple calcination [42-46] up to the hydrothermal conversion [47-49]. Gibbsite activation is a common way to improve reactivity of the industrial products and to conduct the process to the desired final product or to any requested quality of the products. Thus, the simple grinding is an easy way to activate the gibbsite, as well as the bayerite or boehmite [50-52]. Intensifying the activation by larger mechanical energy impact in grinding stage, it is possible to convert the gibbsite directly to α-alumina at lower temperature [53]. Also, the process can be controlled through the cycle gibbsite-boehmite-ceramic oxides, only coupling the mechanical energy impact with adequate temperature values during each stage of conversion [54]. Because the mechanical activation of gibbsite as precursor is made before the thermal treatment [55], the process could be extended with a super activation by attrition [56,57].

Boehmite is a valuable fine precursor. Its simple synthesis consists in decomposition of the sodium aluminate solutions with CO_2, like in modified Bayer process [58]. But, the real first rated precursor requires much more elaborated procedures [59-61]. Even if the boehmite is a processed material with improved properties, some new grades of boehmite have been prepared by over mechanical activation (attrition) of the primary boehmite, obtained by suitable thermal treatments of gibbsite [62]. Also, boehmite, related or not related to Bayer gibbsite, is an aluminum oxy-hydroxide with remarkable applications by itself or as a precursor for different materials used in the catalysis and adsorption domains, where the most well-known intermediary is γ-Al_2O_3 [36][63,64]. The most important investigations of the gibbsite/boehmite dehydroxylation process and the phase transitions mechanisms of new born mineral phases, under various conditions (heating rates, precursors, the thermal and mechanical activation), cover a large aria of extensive researches. All the literature reports are indicating just two paths of individual compounds formed during the thermal transitions from gibbsite to α alumina. Little information is available about the kinetics of dehydroxylation processes and their associated mechanisms [19]. Under high heating rate, the fine gibbsite particles are partially transformed into an amorphous product (ρ-alumina). This intermediate product has a significant higher reactivity and under specific conditions exhibits unusual thermal stability until 800°C [9]. On the contrary, when the heating rate is low or fairly closed to equilibrium conditions, the dehydroxylation and the expected crystalline phases lattice changes are simultaneous taking place, resulting crystalline oxidic compounds (boehmite at temperatures higher than $T > 180°C$, and χ-Al_2O_3 at $T \geq 250°C$) [12]. Actually, the following dynamic factors control all the phase transitions mechanism from Al_2O_3-$3H_2O$ to α- Al_2O_3: temperature and rate of heating, particles size dimension of Al_2O_3-$3H_2O$ before the heating treatments, advanced grinding and the intensive mechanical activation of Al_2O_3-$3H_2O$, as raw material [65]. In the previous works [66,67] have been presented new data about the contributions of both calcination temperature and particles size dimensions upon the different phase transitions with significant changes in crystallinity, and properties of the individual products, emerging after the thermal decomposition of $Al(OH)_3$. The thermal decomposition of crystalline $Al(OH)_3$ was studied over the temperature range of 260°C – 400°C and for particle sizes between 10 and 150 μm. In this work, concerning the aluminum hydroxide thermal activation and activated products physical and mineralogical properties, some data are partially drawn from the previous papers [66, 67]. The new data acquired in this paper, concerning the technical properties of low temperature alumina products, were arranges in such a way to highlighten the contribution of thermal activation, and respectively, the contribution of initial particle sizes, as dynamic factors in conversion of the initial mineral into the final products with industrial uses. This paper is the result of technical and scientifically collaboration between Vimetco SA Tulcea and University Politehnica Bucharest.

II. Material And Methods

Samples preparation

The dried aluminum hydroxide was provided by SC ALUM Tulcea SA, Romania. The selected specimens of dried, milled and classified material are presented in the table 1.

Table 1. Samples particle size dimensions and heating temperature

Samples	Sample S1	Sample S3	Sample S4	Sample S5
Sizes, µm	0 - 150 µm	0 – 20 µm	0 – 10 µm	45 - 150 µm
No heating	S1 25ºC	S3 25ºC	S4 25ºC	S5 25ºC
260 ºC	S1 260ºC	S3 260ºC	S4 260ºC	S5 260ºC
300 ºC	S1 300ºC	S3 300ºC	S4 300ºC	S5 300ºC
400 ºC	S1 300ºC	S3 400ºC	S4 400ºC	S5 400ºC

Additional information regarding the initial specimens of dried aluminum hydroxide are presented in the previous papers [1-3, 66, 67]. Because one purpose of this paper was to point up the importance of particle size distribution (PSD) in the aluminum hydroxide phase transitions, as well as in their amorphisation process, there have been selected only 4 samples, which can rightly exhibit the large difference between them, in terms of particle sizes and PSD (Table 1 and Figure 1). The powders have been firstly dried at 60°C for 24 h, and then calcined at 260°C, 300°C and respectively, 400°C with a heating rate of 5°C/minute, followed by a 3 hours more heating at final temperature. After the heating treatments, the samples were cooled dawn in the oven until room temperature and then weighed, before particle size determination.

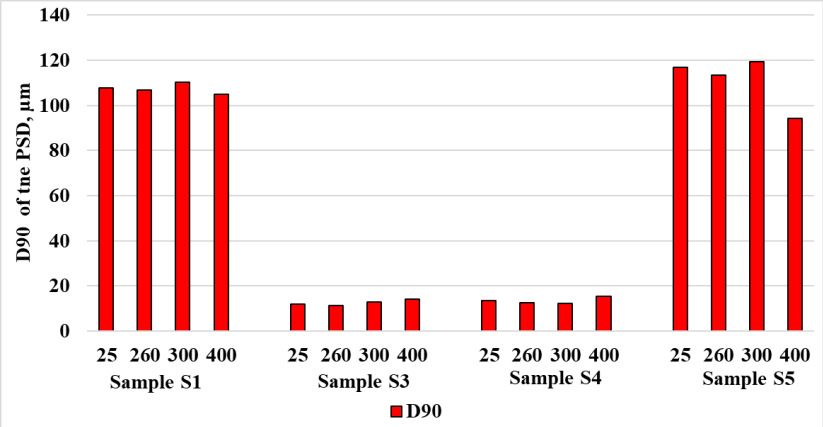

Figure 1. Samples particle size dimension before heating (samples at 25°C) and after heating (samples at 260, 300 and 400°C). The D90 values of the samples PSD

Heating temperature selection

The heating temperature choice is ground on literature data concerning the aluminum hydroxide activation by advanced grinding and on expected changes in the phase transitions mechanism and amorphysation rate. In the figures 2 and 3 are given the thermal analysis diagrams for samples S1 and S3, having very a large differences in their particle sizes (figure 1). Both figures show that the significant expected differences between the mechanisms involved in the first transition of gibbsite (main mineralogical phase in aluminum hydroxide) to other crystalline or amorphous phases did realty taken place. In the figure 2, sample S1, containing larger particles, is shown a first transition process, associated with two successive stages of water loss. In the figure 3, the sample S3, containing smaller particle sizes, presents the same transition process, but only in one single stage.

However, the both single stage and two stages processes produced the same mineralogical phases: boehmite and amorphous gibbsite [67]. Accordingly, for improving and broaden the properties of aluminum hydroxide, amorphous phases partial recrystallization are preferred to be promoted. Thus, the selected temperature values for aluminum hydroxide calcination at low temperatures were laid at 260°C, 300°C and 400°C. In both figures, 2 and 3, it is easy to notice that temperature 260°C is located at the beginning of the first phase transition, where already small water loss had taken place and the material starts the amophisation stage. Temperature 300°C is placed very close to the end of main dehydroxilation stage, where some crystalline or amorphous phases are nucleating and growing. At 400°C, a new phase (usually kappa alumina hydrate) may crystalize or may be partially dehydroxylated, while the material remains amorphous around this temperature.
The same behavior has been observed to the sample S5 (larger particle sizes) and to the sample S4 (smaller particle sizes) from table 1 and figure 1, which partially confirms that particle dimension acts as an active parameter in the aluminum hydroxide phase transitions.

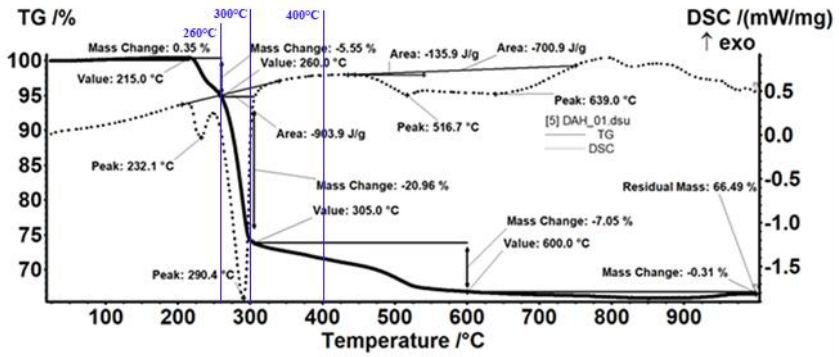

Figure 2. TG/DSC thermal analysis diagram of the sample S 1.

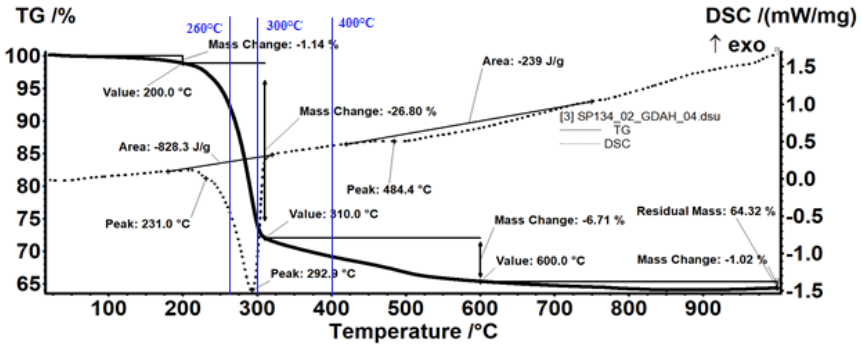

Figure 3. TG/DSC thermal analysis diagram of the sample S 2.

Characterization and Analysis Methods.

Absolute density determination. Materials, which make the subject of this research, have a high fine porosity and a large total volume of pores per cubic centimeter. For acceptable quality measurements of the true density, it has been selected an automatic pycnometer, the Pycnomatic ATC (Thermo Fisher Scientific) equipment, that mainly uses analytical purity helium as test gas. The advantage of using hellium in this kind of determination consists in: high thermal conductivity and ideal gas behavior at room temperature. Integrated calibration procedure is done by a built-in Peltier module (temperature control range: from 18 to 35°C in steps of 0.01°C), required to reach quick sample thermal stability and easiness in the appropriate operations for accurate measurements. Helium has a very small atomic size, and can easily penetrate even to extremely small pores from a solid porous sample, managing to help to a reliable determination of true volume occupied in the sample. The high thermal conductivity of helium and the ideal gas behavior at room temperature make this technique extremely accurate and fast.

Brightness/whiteness degree determinations. The brightness/whiteness degree was measured by two different methods: Method 1. The method uses the NH 310 Portable, Colorimeter, Shenzhen Threenh Technology Co., Ltd. The equipment is provided with built in (white and black) calibration at startup, source of light D65 and the illumination system with LED blue light excitation. The measured color parameters are the CIE Lab coordination indexes, and the degree of brightness/whiteness is computed with the formula: $BD=100- ((100-L)^2+a^2+b^2))^{1/2}$. Method 2 Degree of whiteness measurements, according ISO 2470 and ISO 3688 standards, have been made in blue light (Wb=R457) with the whiteness colorimeter PCE-WSB 1, PCE Deutschland GmbH. The device can find out the brightness level by measuring the intensity of the diffused light reflection on a scale from 1 to 100. The brightness of an absolute black surface is considered equal to 1. The black, white and brilliance standards were used for ensuring accurate and repeatable measurements and consistently results. We have check both methods and decided to use the method 2, because it is more clear-cut and has better repeatability.

Capacity of oil adsorption determination. The oil absorption capacity by the non-heathed and heated aluminum hydroxide at 260 °C, 300 °C, 400 °C, 600 °C, was performed according to ASTM D1483-12 standard "Test Method for Oil Absorption by the Pigments, Gardner- Coleman Method". This method involves the measuring of crude linseed oil volume absorbed by a known mass of particulate material, as a result of gentle mixing and folding until the full saturation point. A mass of aluminum hydroxide sample, equivalent to a volume of 3,0 ± 0,6 ml was accurate weighted and transfered to a glass container. The oil from the burette is added at a flow rate of 1 drop/second, mixing continuously, gently and pliably, the powder with the spatula. It is recommended not to rub or crush the resulting mixture and also, to allow the oil to flow over the dry portions of

the powder. The end point is reached when, with a rolling action of the spatula, the powder accumulates in a single ball or the excess oil contaminates the walls of the glass container. The oil absorption capacity is reported as mL per 100 g dried product..

Water adsoption capacity determination. The ability of a particulate material to absorb water from the air (moisture absorption) is defined by the ratio of the mass of water contained in the material saturated with water (g) (m_2-m_1) to the mass of material in dry state (g) (m_1) (equation 1).

$$W_W = 100\ (m_2 - m_1)/m_1 \qquad (1)$$

where is W_w is the capacity tto absorb water vapors, g H_rO/100 g dry Al $(OH)_3$.

The moisture absorption of a material is dependent on temperature and to relative humidity of the air. A high value of air humidity, associated with a lower temperature, will lead to a higher water vapor absorption capacity, At equilibrium, W_W is the maximum capacity of water absorption. For the experimental determination of water vapor absorption capacity in the case of non-heat treated particles, as well as those heat treated particles at 260ºC, 300ºC, 400ºC and 600ºC, the thermostatic climate chamber Discovery DY110C (ACS) has been used. This climate chamber has the possibility to simulate environments with a temperature varying between -70ºC/+180ºC, with humidity up to 100% or with corrosive chemical agents, in order to determine the quality of analyzed materials and their ability to withstand to various stressing factors. Thus, the materials for analyzes were initially placed for 4 hours in the oven at 105 ºC for absolute drying, then the weighed samples with a mass (m_1) of 1 g ± 0.01 g, have been placed in Petri dishes, and the Petri dishes were laid in the climate chamber. Two sets of parameters were used (simulation conditions): a) temperature 25 and 60 ºC and relative humidity of 50%; and b) 75% relative humidity and 60 ºC temperature. In both cases, the exposure time to the simulated climatic conditions was 24 hours. After completion of the cycle, the samples were weighted, determining the mass of materials saturated with water vapor (m_2).

Other analyses concerning particle size distribution, chemical compositions, TG-DSC thermal analysis, BET and Langmuir specific areas, and porosity determinations have been presented in previous papers [66, 67]. Equipment for particle size dimension determination, solid phase chemical analysis (XRF fluorescence analysis), mineralogical analysis (XRD, diffractometer), TG/DSC thermal analyses, scanning electron microscopy and BET nitrogen absorption surface characterization and pore size analysis have been largely described in the papers [67, 68].

III. Results

Particle size analysis after heating treatment. The figure 1 shows little increases in dimensions of particle, illustrated by D90 parameter for all samples by comparing with the D90 fractions in non-heated samples. That means there are no significant particle breakage or agglomerations during heating and consequently, the initial samples Gauss distribution are preserved over entire heating period. Exception is in the case of sample 5, where the particle size distributions seem to be positively skewed, because the fraction 0-45 μm was removes before the heating process. .Actually, the expansion of the water vapors at the given heating rate was consumed just for pore density growth without significantly affecting the mechanical strength of particles. Also, the figure 1 shows very clearly the great differences in size and particle size distribution between samples S1 and S5, and Sample S3 and S4.

Surface area parameters. The main driving forces in surface area extension of the particulate aluminum hydroxide are the heating rate, final heating point and time length for mineralogical phases stabilization at the end of heating process. It is well known that some other factors may supplementary activate the process or control the precursors number or lines of phase transitions. But, the selection of samples heat treatments and particle size dimension may certainly avoid such a kind of interferences. In order to illustrate the contribution of particle size parameter to the surface extension in aluminum hydroxide particles, five specific parameters, commonly used to describe the both surfaces and particles porosity have been taken into account: P1-BET surface area; P2-BJH Adsorption cumulative surface area of pores between 1.7000 nm and 300.0000 nm; P3-BJH Adsorption cumulative volume of pores between 1.7000 nm and 300.0000 nm, P4-Adsorption average pore width and P5-BJH Adsorption average pore diameter. In the figures 4 and 5 are presented the above mentioned 5 parameters variation with heating temperature and particle size dimension (table 1). Beside the thermal activation, which is clearly more visible at 300°C and 400°C, can be also easily seen, that values for parameters P1-P3 recorded for samples S3 and S4 are obviously higher than the values of the same parameters measured for samples S1 and S5 (figure 4).

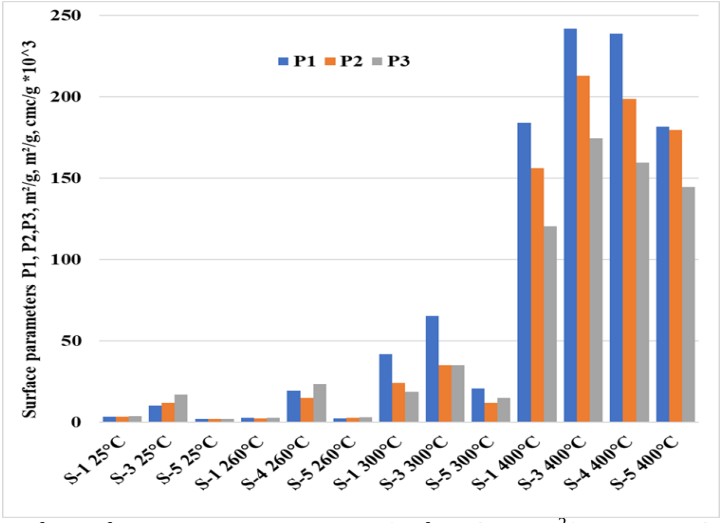

Figure 4. Samples specific surface parameters: P1. BET Surface Area, m^2/g; P2. BJH Adsorption cumulative surface area of pores between 1.7000 nm and 300.0000 nm, m^2/g; P3, BJH Adsorption cumulative volume of pores between 1.7000 nm and 300.0000 nm, cmc/g x 10^{-3}.

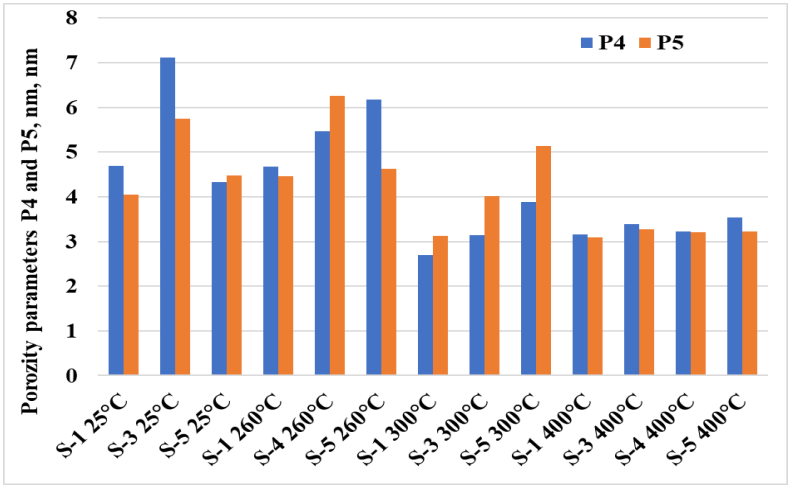

Figure 5. Samples porosity parameters P4. Adsorption average pore width, nm; P5. BJH Adsorption average pore diameter, nm

This assertion is valid even for temperature 25°C (unheated samples), where the gibbsite material activation due to grinding and classification is perceivable. But the real effect of diminishing particle diameter is seen for samples S3 and S4 at 400°C. In this particular case the increase in BET surface for samples S3 and S4 is 20-25% higher than values obtained for samples S1 and S5. Some smaller, but confident increases, have been registered for the BJH adsorption cumulative surface area of pores (parameter P2), and for BJH adsorption cumulative volume of pores (parameter P3). The other 2 parameters, the adsorption average pore width (parameter P4) and the BJH Adsorption average pore diameter (parameter P5), have uneven variations in relation to particle size and temperature, but this variations can be associated with raises in density and declines in the adsorption average pore width, and in the adsorption average pore diameter (figure 5). From the start of heating at 25°C, the smaller particles from sample 3 has both porosity parameters higher then particles with bigger dimensions (S1 and S5 samples). At 260°C this affirmation is still valid only for parameter P5, the adsorption average pore diameter, Also, at 260°C, the parameter P4 grow independently from particles size dimension and mechanical activation by grinding and sieving. In this case, may be the temperature as dynamic factor and respectively, fully perturbation of the crystalline structure of emerging phases (Figure 6) are more appropriate explication for the results at this temperature. Other way, the results at 300°C seem to confirm this hypothesis for both P4 and P5 parameters. Moreover, the results at 400°C show that both porosity parameters P4 and P5 are fully independent on particle sizes.

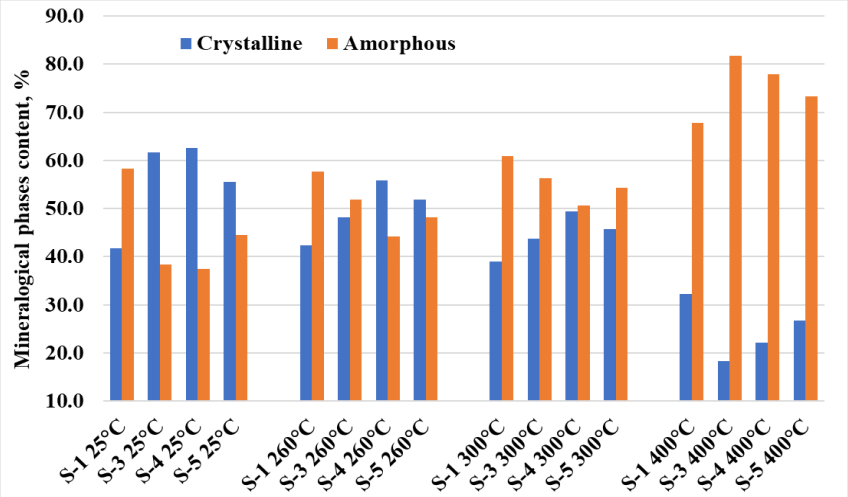

Figure 6. Concentrations of crystalline and amorphous phases:

Actually, these parameters are strongly dependent on the recrystallization of γ-alumina and its associated crystalline phases (Figure 6). According the figure 6, the crystalline phases grow independently of the particle sizes up to 300°C. But, at 400°C and may be to higher temperatures the entire process of amorphization is slightly dependent, also, by particle sizes (Figure 6).

Absolute density. The absolute density is a common parameter, necessary for a complete characterization of all solids and powders products. Determining it by the method of displacing a gas is a fast and reliable way, valid for a wide range of of materials used in technological fields, like: mineralogy, geology, metallurgy, cements and ceramics, abrasives, pharmaceuticals and cosmetics, pigments, catalysts, fibers and polymer materials, and recently also, for battery materials, fuel cells, magnetic material, semi-conductor (CMP) and separation membrane. Density is a parameter of quality control in the high temperature porous and dense alumina ceramics research and production [68]. In the process of densification of high temperature alumina, the alumina hydroxyl compounds as very small particles are releasing nuclei, which contribute to faster growth of dense alumina particles. Also, the absolute density is an important control factor in all the processes designed to produce precursors for both the low temperature alumina transition phases and the special pure alumina products [27]. In the figure 7 are presented the experimental data concerning the effects of temperature and particle size dimensions on the aluminum hydroxide and its low temperature oxy hydrates. At low temperature, all samples density are the same, because are coming from the same batch. At 260°C only sample S3 (0 – 20 microns) has been activate and the density grew up to 2.9 g/cm^3. The other sample remained at the initial level. At 300°C, all the samples ware activated and the densities reached values close to 3.0 g/cm^3, but the higher levels are standing for smaller dimensions samples S3 and S4. The same relative increase in density is valid at 400°C, with the biggest value for sample S3. Thus, the particle dimensions dynamic factor is acting only up to 400°C, when the ratios crystalline/amorphous phases ratio passed a particular threshold.

Whaiteness/Brightness. Whaiteness/Brightness is a quality parameter of a given material defined as the percentage of blue light reflected by the surface of this material from a light source at wavelength of 457 nanometers with the half-peak bandwidth of 44 nm. Due to limitations of the instrumental illuminants and reflected light measurement systems, to capture and measure the intensity of the reflected light, there are no simple correlations between real brightness measurements and data generated by different available experimental methods. Thus, the above whiteness/brightness measurements have to be used, just for comparing and carefully evaluated the brightness of each material individually [69]. Anyway, the results of measurements could be affected by particle size, cristallinity, wetness, compactness and other unexpected properties, even if some new equipment can measure the brightness of pellets, gels, powders, pastes, solids, and liquids. In the figure 8 are presented the brightness data of the experimental samples. From the first series of data, collcted for the samples S1-S5 (60ºC), untill the data series for the same samples at 300ºC, the evidence that the effect attributed to the particle size as driving controlling factor of property named brightness , as a function of particle size is incontestable, because there is a large distance between the S1 and S5 particle diameters and sizes of the S3 and S4 particle diameters. But, this effect is diminishing for the samples heated at 400ºC and 600ºC.

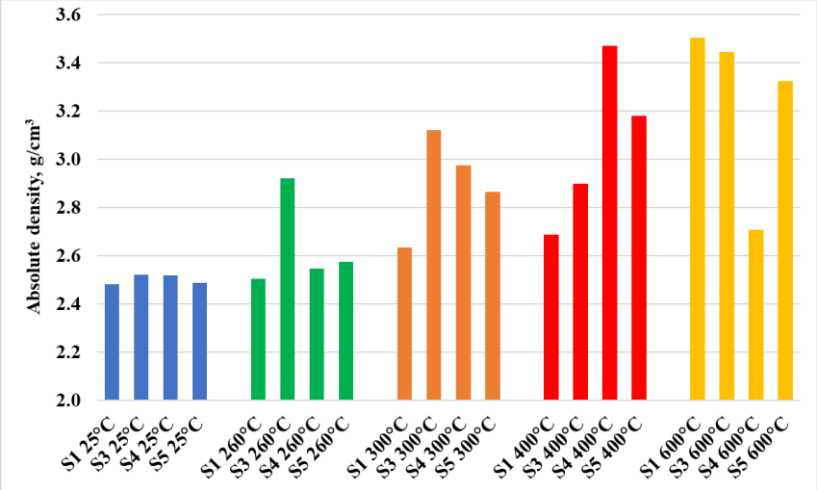

Figure 7. Absolute density of samples

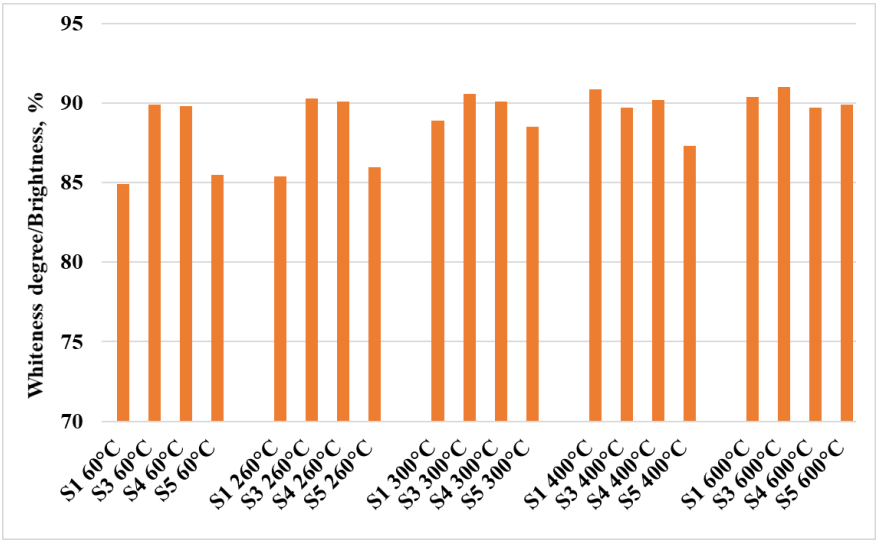

Figure 8. Brightness/Whiteness degree, %.

Correlating the data from figure 8 with data from figure 6 is easy to accept the changings in crystallinity or amorphycity of samples have a real and visible impact on brightness measurements. It is worth to mention the any brightness measurement does not have any connection with colours or shades and, particularly with the whiteness perceived by human eye.

Oil absorption capacity. Oil absorption capacity is a very important property of aluminum hydroxide and its low temperature descending products by thermal dehydroxylation. The technical specifications for different grades products come from their destination as commercial products. Many factors that affect the oil absorption capacity of aluminum oxy-hydrates products like compactness of their structure and specific gravity, surface morphology, crystallinity and particle size distribution are well known. Particle shapes play a significant role in controlling the rate of oil adsorption. Cylindrical grains have a higher oil absorption value than needle-shaped ones or spherical particles, mainly because of the available larger void ratio. The finer particulate materials have the larger specific surface area, and along with the narrower particles size distributions did work out significant increases in the oil absorption capacity. In the figure 9 is given the oil adsorption capacity for the samples enumerated in table 1, heated to 260°C, 300°C, 400°C and 600°C. The effects of the heating temperature and particle size dimension as driving factors in the dehydrixylation processes is clearly seen (the oil capacity is fairly increasing with temperature and predominantly for smaller particle sizes given in the table 1. At 600°C, the slightly decrease in the oil absorption capacity might be attributed to the large growth in concentrations of the amorphous phases in the absorbents samples (figure 6). Aluminum hydroxide and its dehydroxylated compounds uses cover a large area of domains including, absorbents and siccativants, filler, fire retardants, additive and raw materials. For example, in solvent-borne coatings and polymer industries, aluminum hydroxide is one of the best fit additive and flame retarder in many largely used powder coating resin systems: polyester (PE), polyurethane (PU), epoxy (E) and epoxy-polyester (H),

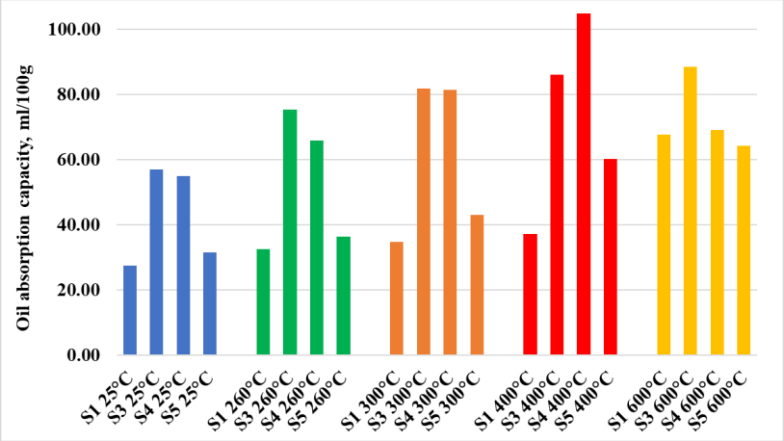

Figure 9. Oil absorption capacity

As flame retardant, aluminum hydroxide prevents burning and emanation of toxic compounds. As additive, aluminum hydroxide contributes to the best adjustments in mechanical and rheological properties of the solvent born coatings, reduces corrosivity and improves the quality of solvent born coats. Fine uniform grades products with D50 around 20 microns and medium oll absorption values (30-40 g/100 g) are highly recommended for this application [16]. Different adsorbents were designed and produced, as reliable adsorbents for oil removal from the water surface. An appropriate adsorbent material must show up high hydrophobicity and hight oleophilicity, low water uptake capacity (high oil/water selectivity), high buoyancy, high oil sorption capacity, low cost and easily availability [69,70]. Figure 9 shows that our low temperature alumina products displays good resemblance in properties connected with oil absorption capacity with above described fillers and with fire retardants used in solvent-borne coatings and in polymer industries. Moreover these products properties might be easily adjusted in the heating treatments, in particle sizes and particles size distribution, in order to match better the required properties. Similar products with low pores size and high specific surface has been used in the treatment of refinery effluent waters containing oil and grease residuals ranging from 50 to 100 mg/L. These residuals were adsorbed onto low temperature calcined alumina products containing gamma alumina as main component, and the fractional removal of oil compounds have brought about large drops in COD and BOD values till 0.57-0.68 mg/L. Absorption mechanism is the chemisorption, and removal percentage rates are increasing with the rise in temperature, due to the released heat. In both cases, γ-alumina structured materials acted as activator factor [71, 72]. Some cited reviews showed that this kind of materials have high potential application in the fields of oil-water separation with real advantages, including strong mechanical properties, rapid sorption rates, high sorbent capacity and interesting applications in the surface chemistry engineering.

Capacity of water vapors adsorption. The results of water vapors adsorption static capacity determinations are presented in the table 2 and in the figure 10. The experimental program encompassed the measurements at the temperature values of 25°C and 60°C, and the air humidity has been 50%, 75% and 95%. It was a minimal program selected for a quick and accurate investigation about the ranges of variation in static capacity of water vapors absorption over some temperature and humidity intervals, for samples of aluminum hydroxide containing mixtures of crystalline and amorphous phases, generated by thermal activation at low temperatures, having well known distinct particle size distributions. At low activation temperature, under 300ºC, all samples exhibited very low water absorption capacity, probably due to no significant changes in specific surface area and porosity. Also, under 300ºC, the deyhdroxilation of gibbsite does not produced enough quantities of new activated phases. Between 300ºC and 600ºC, the experimental materials have been undergoing two real changes in both the mineral phases and their crystallinity (figure 6), with relevant effects on the new activated compounds fundamental properties (figures 4, 5 and 9) [67.68].

Table 2. Capacity of water vapors adsorption

Sample	Sample name	Capacitatea de sbsorbtie a vaporilor de apa, g/100 g probe			
Temperature,		25	25	25	60
Humidity, %		50	75	95	50
GDAH 01 300	S1 300	0.01	0.02	0.00	0.09
GDAH 03-300	S3 300	9.75	9.87	10.85	7.94
GDAH 04-300	S4 300	10.28	10.85	13.45	8.87
GDAH 05-300	S5 300	2.71	4.55	3.30	3.64
GDAH 01 400	S1 400	1.92	2.51	7.53	1.59

GDAH 03 400	S3 400	7.02	8.85	10.21	5.62
GDAH 04 400	S4 400	12.98	16.35	0	9.07
GDAH 05 400	S5 400	10.24	11.72	12.71	7.85
GDAH 01 600	S1 600	5.35	16.81	17.14	3.10
GDAH 03 600	S3 600	9.42	13.77	11.62	6.16
GDAH 04 600	S4 600	0.91	1.10	0.00	0.32
GDAH 05 600	S5 600	4.33	16.50	4.33	3.82

Actually, gibbsite followed its common line of phase transitions: Gibbsite –Boehmite-γ-alumina, associated with large quantities of amorphous phases, with variable crystalline structures (figure 6). The effects of particle size, as driving factor controlling the water absorption capacity, are illustrated in the figure 10, only for the samples heated at 400ºC. As this figure shows, the water absorption capacity is higher for samples S3 and S4 than for samples S1 and S5. This assumption is valid for all temperature values and for any humidity levels in all experiments at 25 ºC and 60 ºC. Some notable drops in water absorption capacities at 600 ºC, even if the predominant phase is γ-alumina accompanied by amorphous phases, might be attributed to the changing in the phase transitions rates at this temperature. For activated alumina, the static water adsorption capacity is the principal parameter for measuring alumina related adsorbents performances as siccativants or metals and organic compounds adsorbents in the water cleaning technologies.

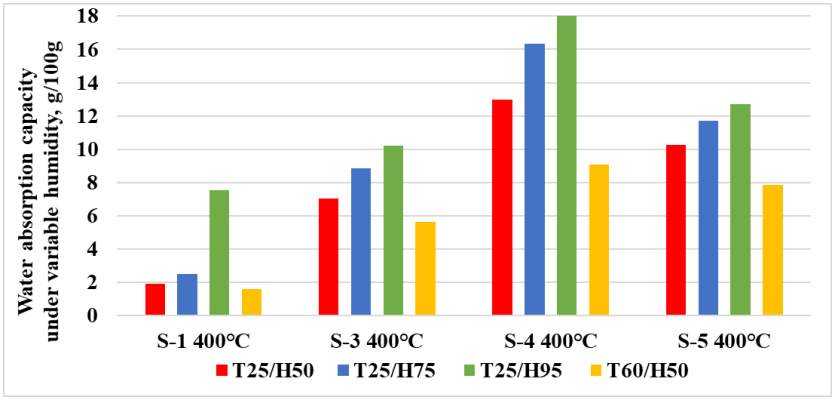

Figura 10. Samples heated at 400°C, Absorption capacity of water vapors under variable humidity, g water/100g: T-Temperature; H-Humidity

The main properties required for such applications are: a) large internal pore volume: b) large value of specific surface; c) controlled pore-size distribution, mostly in the micro-pores range; d) controlled properties of the surface by adding variable functional groups or enlarging the density of active surface sites. Three of these requirements are available for choice in the figures 5 and 6 and in the papers [67, 68]. The fourth of the controlled surface properties factor is represented by the selection of functional groups added during synthesis and finishing or, as usual, in a post processing stages [5, 73]. Al these properties are determined by the structural diversity of polymorphic phases born during low temperature treatments of the aluminum hydroxide (ρ-alumina, boehmite and pseudoboehmitic precursors, γ-alumina, κ-alumina and sometimes η-alumina and χ-alumina, accompanied by their amorphous structures) and depend on the structure and properties of their initial precursors carried by the raw aluminium hydroxide [5, 73].

IV. Conclusions

The thermal decomposition of $Al(OH)_3$ is a very complex process with major crystallographic dislocations and many microstructure reconfigurations on variable lines of phase transitions from precursors to commercial grade products, which come about according to the last well controlled transition, set up as the final stage of entire thermal decomposition process. Many papers and recent reviews have described various kinds of precursors used for preparation and characterization of different activated products with specific properties and applications. In fact, even the crude aluminum hydroxide might be a precursor for some particular mineral phases from the aluminum hydroxide lines of transition or for any of particular properties of a very specific transition phase.

In this paper, as well as in our previous cited papers, the crude aluminum hydroxide, dried, milled and classified has been considered as precursor for the low temperature transition alumina phases, enriched in the amorphous phases, carrying new characteristics and properties. In the previous cited papers, the mechanisms of aluminum hydroxide phase transitions in samples calcined at 260ºC, 300ºC, 400ºC and 600ºC has been studied, as well as the effects of main driving factors (temperature and phase composition) on the chemical and physical

properties of products emerging during thermal treatments at above temperatures, Also, the purity and chemical composition, morphology and specific surface area, pore size, pore distribution and particle size distribution have been analyzed. Beside, some other secondary effects were noticed, like the particle initial size control over mass loss intensities, phase transition rates and degree of crystallinity/amorphicity.

In this paper, the driving factor, the particle initial size, was considered as the reference for analyzing the new data concerning the following technical properties of aluminium hydroxide samples calcined at 260ºC, 300ºC, 400ºC and 600ºC: the absolute density, brightness, oil absorption capacity and water absorption capacity. These last data may suggest new ways for finishing the new emerging hydrated alumina grades and to improve their qualities as adsorbents, fillers, catalyst and catalyst supports, as well as additives for waste water cleaning technologies or additives in the high temperature alumina products industry.

Acknowledgments: *This study was made possible by the implementation of the "Endow the Research and Development Department of SC ALUM SA Tulcea with independent and efficient research facilities to support the economic competitiveness and business development" project, co1funded by the European Regional Development Fund through the Competitiveness Operational Programme 2014–2020. Under this project were purchased and commissioned: "Independent equip1ment/installation for research and development of the technology of wet aluminum hydroxide classification", "Independent equipment/installation for research and development of technology to obtain the dried aluminum hydroxide", and "Independent equipment/installation for research and development of the technology of grinding and screening the dried aluminum hydroxide".*

References

[1]. Dobra G, Iliev S, Cotet L, Boiangiu A, Hulka I, Kim L, Catrina GA, Filipescu L, Heavy metals as impurities in the Bayer production cycle of the aluminum hydroxide from Sierra Leone Bauxite. Preliminary study, J. Sib. Fed. Univ. Engineering and Technologies, *2021*, 14(.2):151-165.
[2]. Dobra G, Garcia-Granda S, Iliev S, Cotet L, Hulka I, Negrea P, Duteanu N, Boiangiu A, Filipescu L, Aluminum hydroxide impurities occlusions and contamination sources, Rev. Chim, 2020. 71(9):65–76.
[3]. Dobra G, Iliev S, Anghelovici N, Cotet L, Filipescu L, Impurities Accumulation on the Surface of Alumina Hydrate Particles in Bayer Technology, Rev. Chim. 2019,70(2): 355-360.
[4]. Dobra G, Kiselev A, Filipescu L,. Alistarh V, Anghelovici N, Iliev S, Full analysis of Sierra Leone bauxite and possibilities of bauxite residue filtration, J. Sib. Fed. Univ. Engeering and. Technology, 2016, 9(5):643-656.
[5]. Meshcheryakov EP, Reshetnikov SI, Sandu MP, Knyazev AS, Kurzina IA,. Efficient Adsorbent-Desiccant Based on Aluminium Oxide, Appl. Sci. 2021, 11(6), 2457.
[6]. Wang L, Shi C, Wang L, Pan L, Zhang X, Zou J, Rational design, synthesis, adsorption principles and applications of metaloxide adsorbents: A review. Nanoscale 2020, 12: 4790–4815.
[7]. Hami H K, Abbas R F, Eltayef E M, MahdiN I, Applications of aluminum oxide and nano aluminum oxide as adsorbents, Review. Samarra J. Pure Appl. Sci. 2020, 2(2):19-32.
[8]. Banerjee S, Dubey S, Gautam R K, Chattopadhyaya M C, Sharma, Y C, Adsorption characteristics of alumina nanoparticles for the removal of hazardous dye, Orange G from aqueous solutions, Arab. J. Chem,, 2019, 12 (8): 5339-5354.
[9]. Kim J, Lee H, Vo H, Lee G, Kim N, Jang S, Joo J, Bead-Shaped Mesoporous Alumina Adsorbents for Adsorption of Ammonia, Materials 2020, 13(6):1375.
[10]. Vahidi G, Bajwa D, Shojaeiarani S, Stark J N, Darabi A., Advancements in traditional and nanosized flame retardants for polymers - A review, J. Appl. Polym. Sci. 2021, 138:1-14.
[11]. Le T H, Hien T, Nguyen, The Influence of Alumina Filler on Mechanical, Thermal and Electrical Properties of Bulk Moulding Compounds (BMCs) Composite, Applied Mechanics and Materials 2019, 889:65–70,
[12]. Saleh M, Al-Hajri Z, Popelka A, Zaidi S J, Preparation and Characterization of Alumina HDPE Composites. Materials (Basel), 2020, 13(1): 250..
[13]. Zheng J, He S, Wang J, Fang W, Xue Y, Xie L, Lin J, Performance of Silicone Rubber Composites Filled with Aluminum Nitride and Alumina Tri-Hydrate, Materials 2020, 13(11): 2489.
[14]. Chen H, Chen K, Yang R, Yang F, Gao W, Use of aluminum trihydrate filler to improve the strength properties of cellulosic paper exposed to high temperature treatment, BioResources 2011,6(3):2399-2410.
[15]. Khan H, Amin M, Ahmad A, Performance evaluation of alumina trihydrate and silica-filled silicone rubber composites for outdoor high-voltage insulations, Turk. J. Elec. Eng. 2018, 26:2688-2700,
[16]. Li W, Yang M, Zhu X, Investigation of the Performance of ATH Powders in Organic Powder Coatings, Coatings 2019, 9(2):110.
[17]. Huim Z, Baowei Y., Shuai Y, Jinbao H, Jixing C, Wei L, Yuanyuan S, Haiping Z, Jingxu Z, Research Status and Development of Functional Powder Coatings, Chemcial Industry and Engineering 2020, 37 (2):1-18.
[18]. Wang Z, Shen X, Yan Y., Qian T., Wang J., Sun Q., Jin C, Facile fabrication of a PDMS/Stearic acid-Al(OH)3 coating on lignocellulose composite with super-hydrophobicity and flame retardancy, Applied Surface Science, 2018, Materials 2018, 11: 727.
[19]. Liu J, Ma Y, Liu W, Song X, Yao S, Wang J., Cheng M, Li, C, Preparation of alumina precursor sols with a high solid content for alumina fibers Materials Research Express, 2019, 6(4):045207.
[20]. Toledo R R, Santoyo V R, Sánchez D M. Merced Martínez Rosales M.M, Effect of aluminum precursor on physicochemical properties of Al_2O_3 by hydrolysis/precipitation method, Nova Scientia, 2018, 10(1):83-99.
[21]. Safaei M, Effect of phase type in the alumina precursor on the flash calcination synthesis, Boletín de la Sociedad Española de Cerámica y Vidrio, 2021.
[22]. Oliveira Notório Ribeiroa J, Vasconcelos D C. L, Vasconcelos, W L, Importance of the Order of Addition of the Alumina Precursor and its Type Into Al-SBA-15 Mesoporous Materials for Use as Water Adsorbents, Materials Research. 2019, 22(1): e20180651.
[23]. Abyzov A M, Aluminum oxide and alumina ceramics (review). Part 1. Properties of Al_2O_3 and commercial production of dispersed Al_2O_3, Refract Ind Ceram 2019, 60:24–32.
[24]. Abyzov A.M, Aluminum Oxide and Alumina Ceramics (Review). Part 2. Foreign Manufacturers of Alumina Ceramics, Technologies and Research in the Field of Alumina Ceramics 2019,.60:33–42.

[25]. Abyzov A.M, Oxide and Alumina Ceramics (Review). Part 3, Russia manufacturers of Alumina Ceramics. 2019, 60:183–191.
[26]. Liu Y, Zhu W, Guan K, Peng C, Wu J, Preparation of high permeable alumina ceramic membrane with good separation performance via UV curing technique, RSC Adv. 2018, 8:13567-13577.
[27]. Souza A D V, Arruda C C, Fernandes L, Antunes M L P, Kiyohara P K,. Salomão R, Characterization of aluminum hydroxide ($Al(OH)_3$) for use as a porogenic agent in castable ceramics, Journal of the European Ceramic Society 2015, 35(2):803-812.
[28]. Kobra Nikoofar K, Shahedi Y, Chenarboo F J, Nano Alumina Catalytic applications in organic transformations, Mini-Reviews in Organic Chemistry 2019, 16(2):102-110.
[29]. Busca G, The surface of transitional aluminas: A critical review, Catalysis Today 2014, 226(1):2-13.
[30]. Busca G, Chapter Three - Structural, surface, and catalytic properties of aluminas, Advances in Catalysis 2014, 57:319-404.
[31]. Busca G, Silica-alumina catalytic materials: A critical review, Catalysis Today 2020, 357:621-629.
[32]. Tregubenko V Y, Belyi A S, Characterization of acid-modified alumina as a support for reforming catalysts, Kinet Catal. 2020, 61:130–136.
[33]. Shirai T, Watanabe H, Fuji M, Takahashi M, Structural properties and surface characteristics on aluminum oxide powders, Annu. Rep. Ceram. Res. Lab. Nagoya Inst. Technol. 2010, 9: 23-3.,
[34]. Coelho, A C V, De Souza Santos H, Kuniiko Kiyoharab P, Pinto Marcos K N, De Souza Santos P, Surface area, crystal morphology and characterization of transition alumina powders from a new gibbsite precursor, Materials Research 2007, 10(2):183-189.
[35]. Egorova S R, Lamberov A A, Effect of the phase composition of gibbsite on the specific surface area of coarse floccule of products formed in its dehydration under thermal treatment, Russ. J. Appl. Chem., 2014, 87(8):1021-1030.
[36]. Ahmadabadi M N, Nemati A, Arzani K, Baghshahi S, The relation between particle size and transformation temperature of gibbsite to α-alumina Miner Process Extr Metall, Trans. Inst. Min. Metall., 2020.
[37]. Baranyai V Z, Kristály F, Influence of grain and crystallite size on the gibbsite to boehmite thermal transformation Studia UBB Chemia, 2015, 9(2):27-44.
[38]. Bruschi L, Mistura G, Nguyen P T, Do, D D, Nicholson D, Park, S J, Lee, W, Adsorption in alumina pores open at one and at both ends, Nanoscale 2015, 7(6):2587-96..
[39]. Vo H,T, Kim J, Kim, N Y, Lee, J K, Joo J B, Effect of pore texture property of mesoporous alumina on adsorption performance of ammonia gas J. Ind. Eng. Chem. 2020, 91:129-138.
[40]. Mehta S K, Kalsotra Murat A M, A new approach to phase transformations in gibbsite: the role of the crystallinity, Thermochim. Acta 1992, 205:191-203.
[41]. Nortier P, Fourre P, Mohammed AB, Saur S O., Lavalley J C, Effects of crystallinity and morphology on the surface properties of alumina Applied Catalysis 1990, 61(1):141-160.
[42]. Van Gog, H. First-principles study of dehydration interfaces between diaspore and corundum, gibbsite and boehmite, and boehmite and γ-Al_2O_3: Energetic stability, interface charge effects, and dehydration defects, Applied Surface Science, 2021(541):1-15.
[43]. Lamouri S, Hamidouche M, Bouaouadja N, Belhouchet H, Garnierd V, Fantozzi G, Trelkat J F, Control of the γ-alumina to α-alumina phase transformation for an optimized alumina densification, Boletín de la Sociedad Española de Cerámica y Vidrio, 2017 56(2):47-54.
[44]. Kovarik L, Bowden M, Andersen A Jaegers N R, Washton N, Szanyi J, Quantification of High Temperature Transition Al2O3 and their phase transformations, Angewandte Chemie International Edition, 2020, 59 (48): 21719-21727.
[45]. Malki A, Mekhalif Z, Detriche S, Fonder G, Boumaza A, Djelloul A, Calcination products of gibbsite studied by X-ray diffraction, XPS and solid-state NMR, J. Solid State Chem, 2014 (215):8-15.
[46]. Day M K B, Hill, V J, Thermal transformations of the aluminas and their hydrates, Nature, 1952,170(4326):539.
[47]. Yamaguchi G, Sakamoto K, Hydrothermal Reaction of Aluminum trihydroxides, Bull. Chem. Soc. Jpn., 1959, 32(7):696-699.
[48]. Sato T, Hydrothermal reaction of alumina trihydrate, J. Appl. Chem, 2007,10(10):414-417.
[49]. Lopushan V I, Kuznetsov G F, Pletnev R N, Kleshev D G, Kinetics of phase transitions of gibbsite during heat treatment in air and in water vapor, Refract. Ind. Ceram, 2007, 48(5):378-382.
[50]. Tsuchida T, Ichikawa N, Mechano-chemical phenomena of gibbsite, bayerite and boehmite by grinding, React. Solids, 1989, 7(3), 207-217.
[51]. Kano J, Saeki S, Saito F, Tanjo M, Yamazaki S, Application of dry grinding to reduction in transformation temperature of aluminum hydroxides, Int. J. Miner. Process, 2000, 60(2):91-100.
[52]. Baranyai, V Z, Kristály F, Szűcs I, Influence of the short time grinding on the thermal decomposition processes of gibbsite produced by the Bayer process, Materials Science and Engineering, 2013, 38(1):15–27.
[53]. Jang S W, Lee H. Y, Lee S. M, Lee S W, Shim K B, Mechanical activation effect on the transition of gibbsite to α-alumina", J. Mater. Sci. Lett, 2000, 19(6):507-510,
[54]. Yong C C, Wang J, Mechanical-activation-triggered gibbsite-to-boehmite transition and activation-derived alumina powders, J. Am. Ceram. Soc, 2001, 84(6):1225-1230.
[55]. MacKenzie K J D, Temuujin J, Okada K, Thermal decomposition of mechanically activated gibbsite, Thermochim. Acta, 327(1-2):103-108.
[56]. Alex T C. Kumar R, Roy S K, Mehrotra S P, Mechanically induced reactivity of gibbsite: Part 1. Planetary milling, Powder Technol, 2014, 264:105-113.
[57]. Alex T C. Kumar R, Roy S K, Mehrotra S P, Mechanically induced reactivity of gibbsite: Part 2. Attrition milling, Powder technology, 2014, 264:229-235.
[58]. Panias D, Paspaliaris I, Boehmite Process-A New Approach in Alumina Production, Erzmetall 2003, 56(2):76-81.
[59]. Ren X, Liu Y, Miao L, Continuous carbonation for synthesis of pseudo-boehmite by using cross-flow rotating packed bed through the reaction of $NaAlO_2$ solution with CO_2 gas, Nanomaterials, 2020, 10(2):263.
[60]. Candela L, Perlmutter D D, Kinetics of boehmite formation by thermal decomposition of gibbsite", Ind. Eng. Chem. Res., 1992, 31(3):694-700.
[61]. Filho R W N D, De Araujo Rocha Montes G C R, Vieira-Coelho A C, Synthesis and characterization of boehmites obtained from gibbsite in presence of different environments, Mater. Res, 2016, 19(3): 659-668.
[62]. Rouquerol J, Rouquerol F, Ganteaume M, Thermal decomposition of gibbsite under low pressures. I. Formation of the boehmitic phase, J Cata,l 1975, 36(1): pp. 99-110.
[63]. Alex T C. Kumar R, Roy S K, Mehrotra S P, Anomalous reduction in surface area during mechanical activation of boehmite synthesized by thermal decomposition of gibbsite, Powder Technol, 2011,208(1):128-136,
[64]. Abdelkader A, Hussien B M, Fawzy E M, Ibrahim A A, Boehmite nanopowder recovered from aluminum cans waste as a potential adsorbent for the treatment of oilfield produced water, Appl. Petrochemical Res, 2021,11:137-146.

[65]. Mohammadi M, Khodamorady M, Tahmasbi B, Bahrami K, and Ghorbani Choghamarani A, Boehmite nanoparticles as versatile support for organic–inorganic hybrid materials: Synthesis, functionalization, and applications in eco-friendly catalysis, Journal of Industrial and Engineering Chemistry. 2021, 97:1-78.
[66]. Isopescu R, Dobra G, Iliev S, Cotet L, Boiangiu A, Filipescu L, Kinetic modelling for thermal decomposition of the aluminum hydroxide dried, milled and classified, U.P.B. Sci. Series B, 2022, 84(2):67-78.
[67]. Vasile B.S, Dobra G, Iliev S, Cotet L, Neacsu I A, Nicoara A I, Surdu V A, Boiangiu A, Filipescu, L. Thermally Activated $Al(OH)_3$: Part I—Morphology and Porosity Evaluation", Ceramics 2021, 4:265–277.
[68]. Vasile B.S, Dobra G, Iliev S, Cotet L, Neacsu I A, Nicoara A I, Surdu V A, Boiangiu A, Filipescu, L. Thermally-Activated Al(OH)3 part II - effect of different thermal treatments, Ceramics 2021, 4:564–575.
[69]. Hubbe M A, Gill, R A, Fillers for papermaking: A review of their properties, usage practices, and their mechanistic role, BioRes. 2016, 11(1):2886-2963.
[70]. Al-Jammal N, Juzsakova T, Review on the effectiveness of adsorbent materials in oil spills clean up, 7th International Conference of ICEEE, 17-19 of November 2016, Budapest, Hungary [Publication year: 2017:131-138.
[71]. Norisetty A, Basu J K, Sengupta S, Application of alumina to oil and grease removal from refinery effluent hydrol, Current Res, 2011, 2 (4):1-4.
[72]. Lamouria S, Hamidoucheb M, Bouaouadja N, Belhoucheta, H, Garnierd, V, Fantozzi, G, Trelkate J F, Control of the γ-alumina to α-alumina phase transformation for an optimized alumina densification, Boletín de la Sociedad Española de Cerámica y Vidrio, 2017, 56(2)"47-54.
[73]. Zotov R A, Glazyrin A A, Danilevich V V, et al. Influence of the temperature of calcination of bayerite-containing aluminum hydroxide pellets on the water vapor adsorption capacity and acid-base properties of alumina, Kinet Catal 53:570–576.

Gheorghe Dobra, et. al. "Technical Properties and Uses of the Aluminum Hydroxide, Dried, Milled and Classified." *IOSR Journal of Applied Chemistry (IOSR-JAC)*, 15(06), (2022): pp 10-22.